

Performance of LS-DYNA® Concrete Constitutive Models

Youcai Wu, John E. Crawford, Joseph M. Magallanes

Karagozian & Case, 2550 N Hollywood Way, Suite 500, Burbank, CA 91505

Abstract

LS-DYNA provides several constitutive models for concrete. To provide some guidance in selecting a proper one for users who have limited experience on concrete, this paper reviews the background theory and evaluates the performance of three popular ones, namely, MAT072R3 (KCC), MAT084 (Winfrith), and MAT159 (CSCM). The basic performance of concrete constitutive models in capturing key concrete behaviors, such as post-peak softening, shear dilation, confinement effect, and strain rate enhancement, is examined through single element simulations including both uniaxial and triaxial load paths. Subsequent to this presentation, the models are applied in analyzing structures subjected to quasi-static, blast, and impact loads and the responses are compared with available test data in order to investigate their capability to predicting and reproducing actual structural responses.

Keywords: concrete, constitutive models, KCC, Winfrith, CSCM

1 Introduction

Concrete is a very common material in modern civil constructions, such as highways, bridges, skyscrapers, etc. The safety of these structures under blast, impact, and ballistic loads has been one of the primary concerns of designers in recent years. However, full-scale structural response test data is costly and difficult to obtain for these types of loads. As a consequence, responses predicted by physics-based numerical analyses have been important resources for both academics and structural engineers to determine the behaviors of reinforced concrete (RC) structures under these loads. Consequently, practitioners are continuously looking for verified and validated numerical models, so that consistent sets of virtual response data can be generated, and, from which one can study structural behaviors, formulate simplified engineering models, and develop new structural and material designs to have improved resistance to these loads.

To realistically predict the behaviors of RC structures under various types of loads, the concrete constitutive model needs to be shown to simulate known behaviors at smaller material specimen levels up to the full-scale structural level. Although it is very difficult to predict the behavior of concrete exactly, the constitutive model should capture the most basic behaviors of concrete. Advances in finite element (FE) methods and material constitutive modelings have made it feasible to support engineers' daily requirements in designs and assessments.

Among the readily available FE softwares, LS-DYNA® is widely applied in analyzing structural responses to shock and impact loads, and it provides a variety of concrete constitutive models, such as Mat_Pseudo_Tensor (MAT016), Mat_Geologic_Cap_Model (MAT025), Mat_Concrete_Damage (MAT072), Mat_Soil_Concrete (MAT078), Mat_Winfrith_Concrete (MAT084), Mat_Brittle_Damage (MAT096), Mat_Johson_Holmquist_Concrete (MAT111), Mat_CSCM_Concrete (MAT159). Each of these models has its own advantages and disadvantages, therefore, FE analysts are actually facing a wide range of choices but they may

only have very limited experience or background knowledge on concrete to be based upon to select the most appropriate model.

The primary purpose of this paper is to facilitate some guidelines for users who don't have much experience or knowledge on concrete to select a proper constitutive model for their analyses and designs. This is done through reviewing the background theory and evaluating the performance of three of the many LS-DYNA concrete constitutive models, i.e., MAT072 [1, 2, 3, 4], MAT084 [5, 6], and MAT159 [7, 8]. One common advantage of these models is that their keyword input is relatively simple. The models are first applied in single element simulations to show their capability in capturing the key concrete behaviors, such as post-peak softening, shear dilation, and confinement effects. The models are then applied in solving several structural problems under different loading conditions, including, quasi – static, blast, and impact loads. These numerical responses are compared with available test data so to assess the effectiveness of each model in reproducing structural responses. The code used for the numerical studies is LS-DYNA R4.2.1, Revision 53450, released on 6/08/2009 and simple inputs are used for all the material models.

2. Theoretical Background

Concrete is a pressure dependent material, therefore, the general form of the yield function can be written as:

$$Y(I_1, J_2, J_3) = 0 \quad (1)$$

where I_1 is the 1st invariant of stress tensor, which represents volumetric responses; J_2 and J_3 are the 2nd and 3rd invariants of deviatoric stress tensor and they account for deviatoric responses. In general, the primary difference between various concrete constitutive models is how the deviatoric and volumetric responses are characterized.

2.1. Karagozian & Case Concrete (KCC) Model – MAT072

Intended for analyzing RC structural responses to blast and impact loadings, the KCC model was initially developed in early 1990s in DYNA3D and was ported to LS-DYNA in 2004. This model allows automatic generation of all the parameters by inputting only the unconfined compressive strength and density of the concrete. It has been applied in analyzing many RC structures subjected to quasi-static, blast, and impact loads [5, 9, 10]. A comprehensive model review and validation application is provided in Reference [11].

The KCC model has three independent strength surfaces and they can be formulated in a generalized form as:

$$F_i(p) = a_{0i} + \frac{p}{a_{1i} + a_{2i}p} \quad (2)$$

where i stands for y, m, r , i.e., the yield strength surface, the maximum strength surface, and the residual strength surface, and $p = -I_1/3$ is the pressure. a_{ji} ($j = 0, 1, 2$) are parameters calibrated from test data (the default parameters are based on data presented in Reference [12]).

The failure surface is interpolated between the maximum strength surface and either the yield strength surface or the residual strength surface according to the following form:

$$F(I_1, J_2, J_3) = \begin{cases} r(J_3) [\eta(\lambda)(F_m(p) - F_y(p)) + F_y(p)] & \lambda \leq \lambda_m \\ r(J_3) [\eta(\lambda)(F_m(p) - F_r(p)) + F_r(p)] & \lambda > \lambda_m \end{cases} \quad (3)$$

Here λ is the modified effective plastic strain or the internal damage parameter, which is a function of J_2 and other parameters (such as damage evolution parameter, hardening parameter). $\eta(\lambda)$ is a function of the internal damage parameter λ , with $\eta(0)=0$, $\eta(\lambda_m)=1$, and $\eta(\lambda \geq \lambda_{\max})=0$. This implies that the failure surface starts at the yield strength surface, and it reaches the maximum strength surface as λ increases to λ_m , and then it drops to the residual surface as λ further increases up to λ_{\max} . λ_m , λ_{\max} , and $\eta(\lambda)$ relationships are calibrated from experimental data. $r(J_3)$ is a scale factor in the form of William – Warnke equation [13], which introduces the dependence to J_3 so that brittle (under low confinement) to ductile transition (under high confinement) is properly modeled.

In addition, to represent the behavior of RC walls subjected to in-plane constraints and out-of-plane blast loads more accurately, the plastic flow of the KCC model is allowed to be partially associative, so that the model can be partially associative, fully associative and non-associative. The plastic flow function is defined as:

$$g = \sqrt{3J_2} - \omega F(I_1, J_2, J_3) \quad (4)$$

where ω is the associativity parameter (0 for non-associative, 1 for fully associative).

2.2. Winfrith Concrete Model – MAT084

The Winfrith concrete model (MAT084) was developed in 1980s, intended in solving RC structures subjected to impact loadings, and was implemented into LS-DYNA in 1991. Although the input is not as simple as the KCC model, its keyword input is still relatively simple and does not need much knowledge on concrete. Another appealing feature of this model is that it allows up to three orthogonal crack planes per element and the cracks can be reviewed through LS – Prepost. This model has mainly been applied in obtaining responses of RC structures subjected to impact loadings [6, 14, 15].

The Winfrith concrete model is based upon the so called four parameter model proposed by Ottosen [13, 16]:

$$Y(I_1, J_2, J_3) = aJ_2 + \lambda\sqrt{J_2} + bI_1 - 1 \quad (5)$$

with

$$\lambda = \begin{cases} k_1 \cos \left[\frac{1}{3} \cos^{-1} (k_2 \cos(3\theta)) \right] & \cos(3\theta) \geq 0 \\ k_1 \cos \left[\frac{\pi}{3} - \frac{1}{3} \cos^{-1} (-k_2 \cos(3\theta)) \right] & \cos(3\theta) \leq 0 \end{cases} \quad (6)$$

$$\cos(3\theta) = \frac{3\sqrt{3}}{2} \frac{J_3}{J_2^{3/2}} \quad (7)$$

The four parameters, i.e., a, b, k_1 , and k_2 , are functions of the ratio of tensile strength to compressive strength (f_t / f'_c), and they are determined from uniaxial compression (correspondingly, $\theta = 60^\circ$), uniaxial tension ($\theta = 0^\circ$), biaxial compression ($\theta = 0^\circ$), and triaxial compression ($\theta = 60^\circ$) tests.

2.3. Continuous Surface Cap (CSC) Model – MAT159

Aimed at roadside safety analyses, the CSC model was developed in 1990s and was made available in LS-DYNA around 2005. Similar as the KCC model, automatic generation of all the parameters is allowed by this model. A comprehensive model review and validation application of this model can be found in References [17, 18].

The CSC model combines the shear (failure) surface with the hardening compaction surface (cap) by using a multiplicative formulation. The yield function is defined in terms of three stress invariants proposed by Schwer and Murray [7] and Sandler et al [8]:

$$Y(I_1, J_2, J_3) = J_2 - \mathfrak{R}(J_3)^2 F_f^2(I_1) F_c(I_1, \kappa) \quad (8)$$

where $F_f(I_1)$ is the shear failure surface, $F_c(I_1, \kappa)$ is the hardening cap with κ to be the cap hardening parameter, and $\mathfrak{R}(J_3)$ is the Rubin three – invariant reduction factor [19]. The multiplicative form allows the cap and shear surfaces to be combined continuously and smoothly at their intersection.

The shear failure surface $F_f(I_1)$ is defined as:

$$F_f(I_1) = \alpha - \lambda \exp^{-\beta I_1} + \theta I_1 \quad (9)$$

The material constants α, β, λ , and θ are determined from triaxial compression test data.

The cap hardening surface is expressed as:

$$F_c(I_1, \kappa) = \begin{cases} 1 - \frac{(I_1 - L(\kappa))^2}{(X(\kappa) - L(\kappa))^2} & I_1 \geq L(\kappa) \\ 1 & I_1 \leq L(\kappa) \end{cases} \quad (10)$$

$$L(\kappa) = \begin{cases} \kappa & \kappa \geq \kappa_0 \\ \kappa_0 & \kappa \leq \kappa_0 \end{cases} \quad (11)$$

$$X(\kappa) = L(\kappa) + R F_f(I_1) \quad (12)$$

Eq.(10) depicts the ellipse (or cap) for $I_1 \geq L(\kappa)$. The shear failure surface intersects the cap at $I_1 = L(\kappa)$. κ_0 is the value of I_1 when the shear surface and the cap intersect initially (before cap expands or shrinks). The cap expands (i.e., $X(\kappa)$ and κ increase) when plastic volume

compaction occurs, and the cap shrinks (i.e., $X(\kappa)$ and κ decrease) when plastic volume dilation occurs. The motion of the cap is controlled by the hardening rule specified by:

$$\varepsilon_v^p = W \left[1 - \exp^{(-D_1(X-X_0)-D_2(X-X_0)^2)} \right] \quad (13)$$

where ε_v^p is the plastic volumetric strain, W is the maximum plastic volumetric strain, X_0 is the initial location of the cap when $\kappa = \kappa_0$. The five parameters, X_0, R, W, D_1, D_2 , are determined from hydrostatic compression and uniaxial strain tests.

3. Stress Path Analysis Using Single Elements

The basic performances of the concrete constitutive models are examined through single element simulations subjected to various stress paths similar to that done previously by Magallanes [20]. In these tests, three neighboring faces of the element are defined as symmetry planes so that the other three surfaces can move in their normal directions without any constraint from essential boundary conditions, if otherwise applied.

The tests performed are unconfined uniaxial compression (UUC), unconfined uniaxial tension (UUT), and triaxial compression (TXC) tests. The unconfined compressive strength of the concrete is 45.4 MPa and its maximum aggregate size is 19 mm.

3.1. Unconfined Uniaxial Compression (UUC) and Tension (UUT) Tests

The stress-strain curves for single element UUC and UUT tests are shown in Figure 1 and Figure 2, respectively. It is observed that the KCC model predicts elastic – (very little hardening) plastic – softening response, the CSC model predicts elastic – softening behavior, and they are consistent with test observations [12]. However, the Winfrith model predicts an elastic – perfect plastic response in compression, and very slow strain softening in tension. This is not physical for concrete. The results also reveal that both the KCC and CSC model can model shear dilation phenomenon (volumetric strain in Figure 1: positive for compaction and negative for expansion), but the Winfrith model does not. The shear dilation is critical for confinement effect in reinforced concrete. For example, in steel stirrup or fiber reinforced polymer reinforced concrete, axial force (in these reinforcements) will be built up due to dilation and the concrete will be confined by these reinforcements. The Winfrith model will not be able to predict this effect.

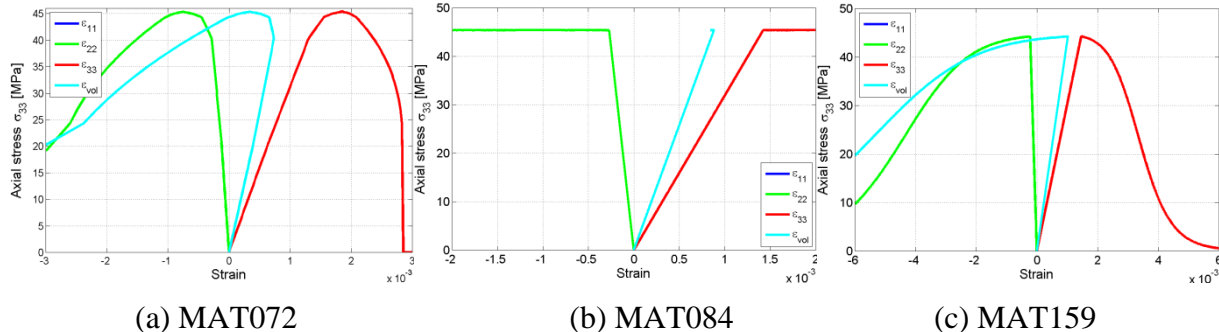


Figure 1. Stress – strain relationships for single element UUC tests

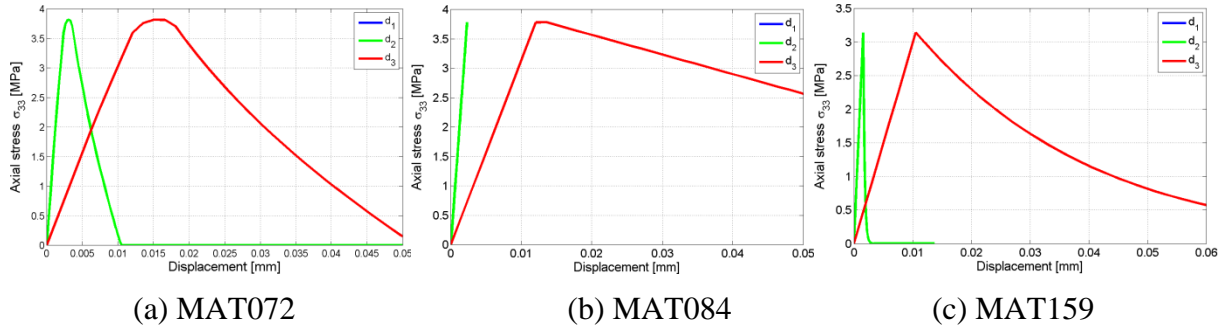


Figure 2. Stress – strain relationships for single element UUT tests

3.2. Triaxial Compression (TXC) Tests

Figure 3 describes the principal stress difference (i.e., engineering axial stress minus confinement pressure) – net strain (i.e., total engineering strain minus the part due to hydrostatic loading phase) curves for TXC tests, where solid lines represent axial strain versus stress difference, dashed lines stand for lateral strain versus stress difference, and the legend indicates confinement pressure. The brittle – ductile transition, from low to high confinement level, is correctly resolved by both the KCC and CSC model. Since there is no softening in compression for the Winfrith model, there is no brittle – ductile transition evident from this model. The figure also demonstrates that the KCC model is stable for any level of confinement, whereas the Winfrith and CSC model is only stable for almost no confinement. It is worth pointing out that the confinement here is applied explicitly as surface pressures, which is the reason that the Winfrith model exhibits some form of confinement effects. Because the Winfrith model cannot model shear dilation effect, structural models will not implicitly capture confinement, as is demonstrated in the following examples.

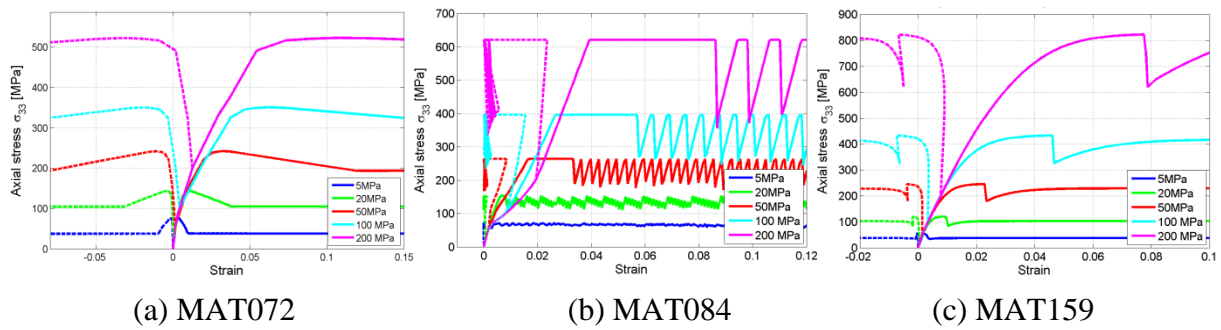


Figure 3. Stress – strain relationships for single TXC tests

4. Predicting and Reproducing Structural Responses

The performances of the concrete constitutive models on structural applications are evaluated in this section. Several structures subjected to various types of loads, namely, quasi – static, blast, and impact loads, are analyzed and compared with available test data.

4.1. Triaxial Compression Test of Solid Cylinder

The solid, plain concrete cylinder used in the test has a dimension of 6-inch (152.4 mm) diameter and 12-inch (304.8 mm) height and the concrete has an unconfined compressive strength of 45.4 MPa. The geometry and boundary conditions are shown in Figure 4. Once again, the confinement is applied explicitly by surface pressure in this example.

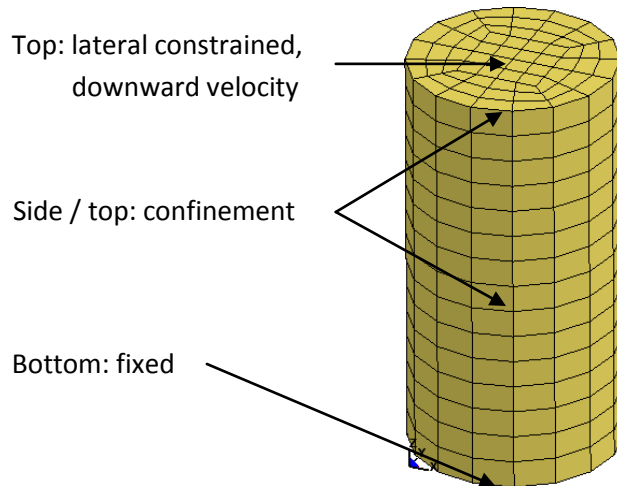


Figure 4. Model of TXC test

Figure 5 presents the engineering stress difference versus net engineering axial strain for various simulations, and they are compared with the test data [12]. Solid lines are the numerical results, dashed lines are the test data, and the legend indicates the confinement pressure. The results indicate that the KCC model can catch the peak strength, post-peak softening, and brittle – ductile transition from low to high confinement, and it agrees well with the test data. On the other hand, the Winfrith model can approximately obtain the peak strength, but no post – peak softening and no brittle – ductile transition regardless of confinement pressure. The CSC model can only approximately match the test data for no confinement case, and the numerical response is unstable for high confinement cases and does not match even just the peak strength.

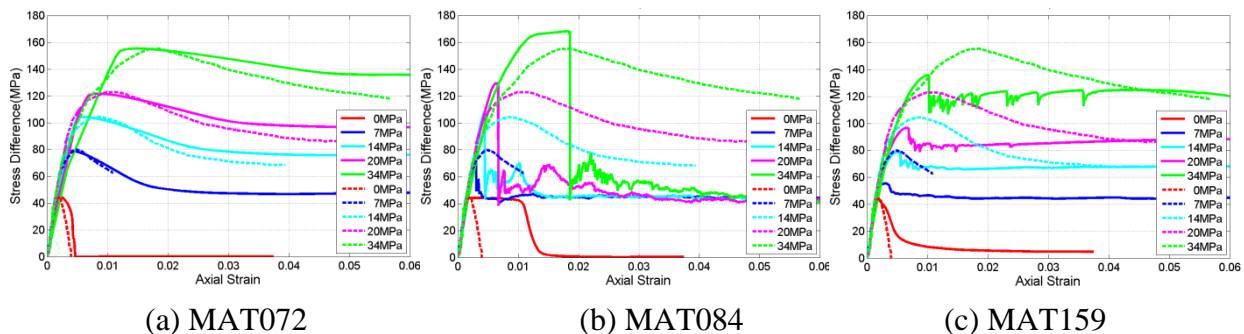


Figure 5. Stress – strain relationships for structural TXC tests

4.2. Cylinder Implosion Test

As shown in Figure 6, a plain concrete cylinder with outer diameter of 16-inch (406.4 mm) and wall thickness of 1.01-inch (25.65 mm) is used in the implosion test. In the test, a uniform gradually increasing pressure is applied on the outer surface until the cylinder implodes and the test results can be found in Reference [21]. The concrete has an unconfined compressive strength of 42.3 MPa. It should be pointed out that, according to the test report [21], 5% initial out-of-roundness is applied to the cylinder. This means that the cross – section of the cylinder is not a circle but an ellipse, and the ratio of the length of short axis to long axis is 0.95.

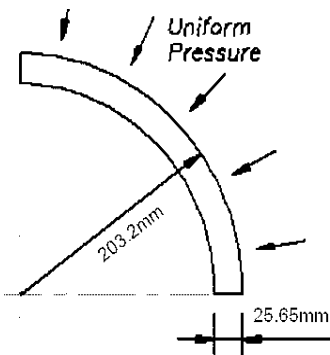


Figure 6. Geometry of cylinder implosion test

The cylinder is considered to be infinitely long so that plane strain boundary condition can be applied (see Reference [21] for detailed discussions). Due to symmetry, only a quarter of the cylinder is modeled. In the laboratory test [21], the pressure rises up 0.012 MPa/sec, which is too slow to model exactly in LS-DYNA for this numerical study (it would cost 2.5-month for a 1,600-element model with 4CPUs). Therefore, the loading speed in simulation is 13.8 MPa/sec for two scenarios, which are with, and without strain rate enhancement, respectively. It is believed that the result without strain rate enforcement should be closer to the test since the actual test is quasi – static.

Figure 7 sketches the relationship between the radial displacement and applied outer pressure. The legend with “NR” refers to no strain rate enhancement and “RT” for strain rate enhanced case. The curve plateaus at a certain radial displacement and implies the implosion pressure. The KCC model without strain rate enhancement is observed to predict a very close result to the test. The prediction by the Winfrith model with strain rate enforcement agrees well with the test. On the other hand, no clear plateau point is seen on the CSC model result. This suggests that the response predicted by the CSC model has too much “ductility”.

In addition, Figure 7 demonstrates that the strain rate effect [22, 23] is represented clearly in the KCC and Winfrith model. Although there is no significant difference between with and without rate enhancement cases for the CSC model, the model does predict some rate effect, probably calibrated differently from the KCC and Winfrith model.

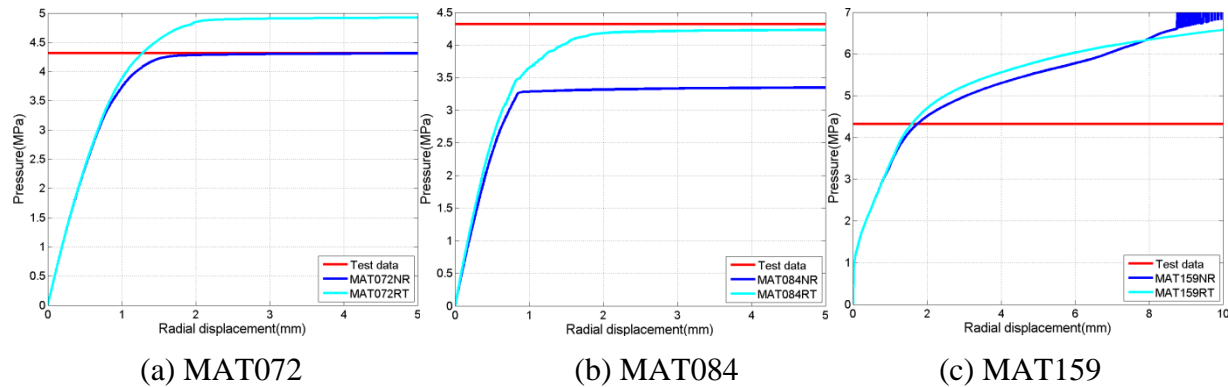
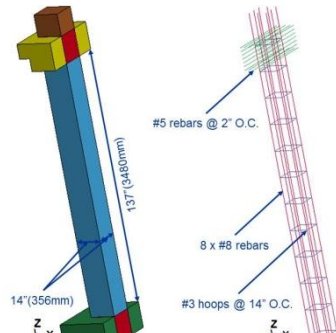


Figure 7. Radial displacement – applied pressure curves for cylinder implosion test

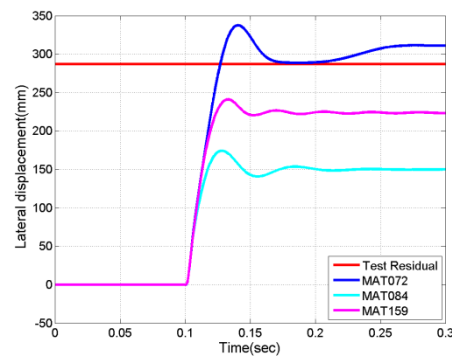
4.3. Reinforced Concrete (RC) Column Subjected to Blast Load

A cross – section of 14-inch by 14-inch (356 mm by 356 mm) reinforced concrete column is subjected to the blast loads generated from a nearby bare high explosive charge [4, 25]. The geometry of the column is shown in Figure 8 (a). The unconfined compressive strength of the concrete is 45.0 MPa, and the steel reinforcement is ASTM Grade 60.

The blast load applied on the front face of the column is the actual pressure recorded during the field test. In the test, the column sustained a shear failure early, which leads to a large – deformation tensile membrane response. As a result, the column deformed about 280 mm laterally, but did not break free from the building as shown in Figure 9 (a). Figure 9 also shows the damage distribution computed by the three constitutive models. The color of the fringes indicates the level of damage (effective plastic strain for MAT084). The KCC model is able to predict the overall deformation of the column correctly, the Winfrith model cannot pick up the localized shear failure on the column, and the CSC model calculates an erroneous localized shear failure at approximately $\frac{1}{4}$ column height. Figure 8 (b) compares the lateral displacement at the column’s mid-height. This figure expresses that the response predicted by the KCC model can match test data, and the responses predicted by the Winfrith and CSC model are too stiff.



(a) Geometry



(b) Lateral deflection at mid-height column

Figure 8. RC column subjected to blast loads

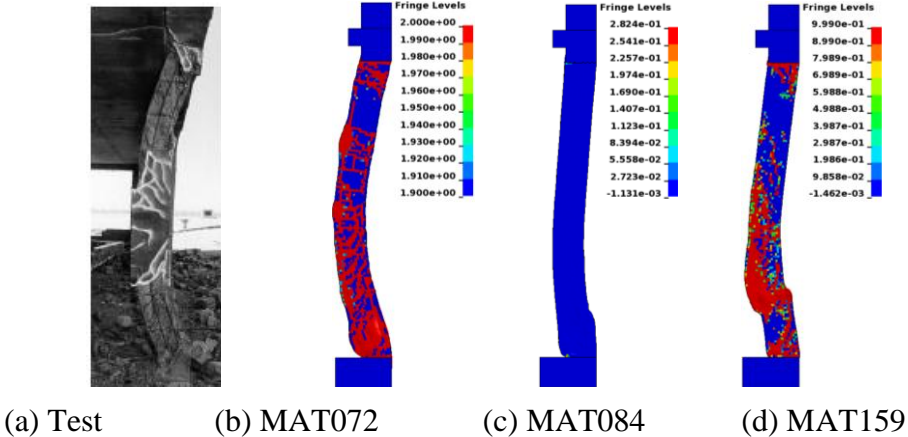


Figure 9. Damage distribution of RC column subjected to blast loads

4.4. Reinforced Concrete (RC) Slab Subjected to Impact Load

A scale model test [26] of aircraft impact on RC panel is investigated in this section. The dimension of the panel is 60 mm thick and 1.5 m by 1.5 m wide. The panel is constructed by unconfined compressive strength of 31.4 MPa concrete and reinforced by D3 rebars at 25 mm on center each face each way. To model the perforation, material erosion is applied. The yield strength of rebar is 300 MPa and its failure strength is 380 MPa. The aircraft has a total mass of 25.25 kg and moves at 142 m/sec toward the center of the panel, as shown in Figure 10 (a). More details about the test can be found in Reference [26].

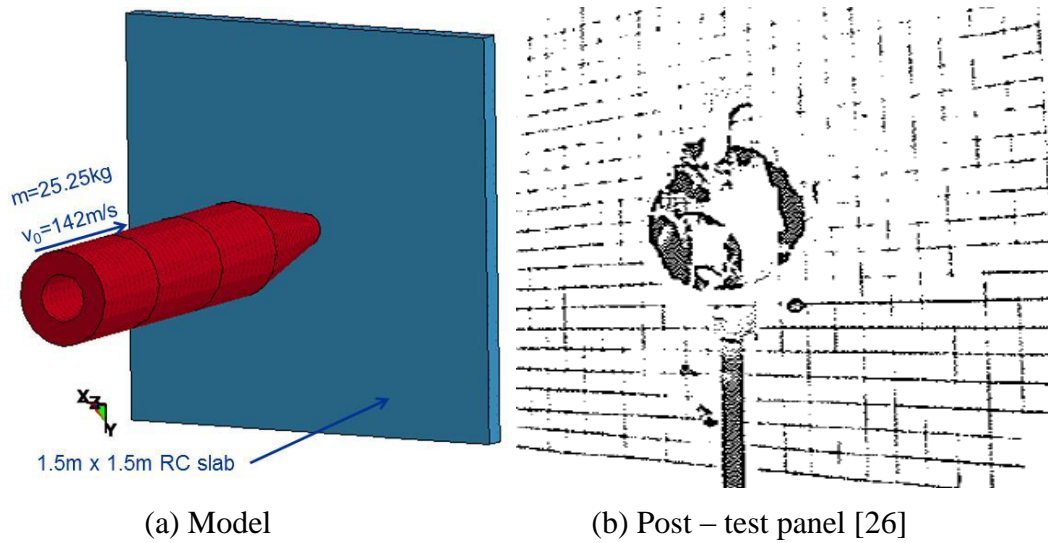


Figure 10. Model and post – test panel

Figure 11 shows the velocity history (the test data is digitized from Reference [26]) on aircraft and Figure 12 shows the deformed panel at termination. The actual test shows perforation on the RC panel after penetration [26] as shown in Figure 10 (b), the aircraft has a

residual velocity of 82 m/sec. The figure indicates that the residual velocity predicted by the KCC and CSC model matches test data very well, whereas the response predicted by the Winfrith model is so stiff that it completely stopped the aircraft. The deformed shape shown in Figure 12 explains that both the KCC and CSC model captures the perforation, but the Winfrith model cannot.

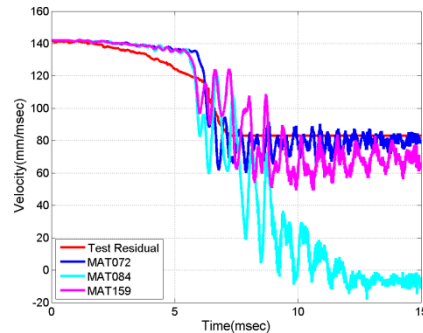


Figure 11. Engine velocity of aircraft – RC panel impact test

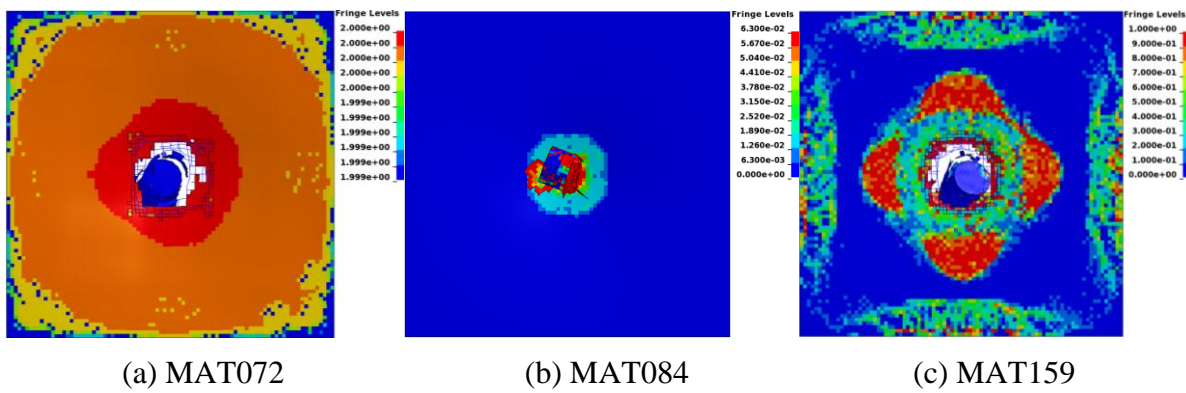


Figure 12. Damage distribution of aircraft – RC panel impact test

5. Conclusion Remarks

This paper reviews the theory and examines the performance of three concrete constitutive models provided by LS-DYNA, namely, the Karagozian & Case concrete model (the KCC model, or MAT072R3), the Winfrith concrete model (MAT084), and the continuous surface cap model (CSCM, or MAT159). These models are all three - invariant isotropic plasticity models and they all take relatively simple input.

The KCC model (MAT072R3) can capture the key concrete behaviors including post - peak softening, shear dilation, confinement effect, and strain rate effect properly. Structural analyses also show that the KCC model is suitable for quasi – static, blast, and impact loads.

The Winfrith model (MAT084) can model post - peak softening in tension but not compression. It can also simulate strain rate effect and confinement effect (with explicit pressure only). An attractive feature of MAT084 is that it allows up to three orthogonal crack planes per

element and the cracks are viewable through LS – Prepost. However, the Winfrith model cannot represent shear dilation, therefore, the confinement effect exerted by reinforcement, such as steel stirrups and fiber reinforced polymer (FRP) wraps, will not be predicted correctly with this model.

The CSC model (MAT159) can model damage – based softening and modulus reduction, shear dilation, shear compaction, confinement effect, and strain rate effect. However, this model works well only for low confinement situations. The strain rate effect in CSC model is calibrated quite differently from the KCC and Winfrith model.

References:

1. Malvar, L.J., Crawford, J.E., Wesevich, J.W., and Simons, D. "A new concrete material model for DYNA3D," TM-94-14.3, Report to the Defense Nuclear Agency, Karagozian and Case, Glendale, CA, October 1994
2. Malvar, L.J., Crawford, J.E., Wesevich, J.W., and Simons, D. "A plasticity concrete material model for DYNA3D," *International Journal of Impact Engineering*, vol. 19, p847-873, 1997
3. Malvar, L.J., Crawford, J.E., Wesevich, J.W., and Simons, D. "A new concrete material model for DYNA3D - Release II: shear dilation and directional rate enhancements," TM-96-2.1, Report to the Defense Nuclear Agency, Karagozian and Case, Glendale, CA, January 1996
4. Magallanes, J.M., Wu, Y., Malvar, L.J., and Crawford, J.E. "Recent Improvements to Release III of the K&C Concrete Model", Proceedings of the 11th International LS-DYNA® Users Conference, Dearborn, MI, June 6-8, 2010
5. Broadhouse, B.J. "DRASTIC – A computer code for dynamic analysis of stress transients in reinforced concrete," Safety & Engineering Science Division, AEE, Winfrith, AEEW – R2124, 1986
6. Broadhouse, B.J. "The Winfrith concrete model in LS-DYNA3D," Safety Performance Department, Atomic Energy Authority Technology, Winfrith, SPD/D(95)363, February, 1995
7. Schwer, L.E., and Murray, Y.D. "A three-invariant smooth cap model with mixed hardening," *International Journal for Numerical and Analytic Methods in Geomechanics*, vol. 18, p657-688, 1994
8. Sandler, I.S., DiMaggio, F.L., and Baladi, G.Y. "Generalized cap model for geological materials," *ASCE Journal of the Geotechnical Division*, vol. 102, p683-699, 1976
9. Malvar, L.J., Wesevich, J.W., and Crawford, J.E. "Procedures for including fragment loading and damage in the response predictions of reinforced concrete slabs," Eighth International Symposium on Interaction of the Effects of Munitions with Structures, McLean, VA, April 1997
10. Crawford, J.E., Malvar, L.J., Wesevich, J.W., Valancius, J., and Reynolds, A.D. "Retrofit of reinforced concrete structures to resist blast effects," *ACI Structural Journal*, vol. 94, p371-377, 1997
11. Crawford, J.E., Magallanes, J.M., Lan, S., and Wu, Y. "User's manual and documentation for release III of the K&C concrete material model in LS-DYNA," TR-11-36-1, Technical Report, Karagozian & Case, Burbank, CA, November, 2011
12. Joy, S., and Moxley, R. "Material characterization, WSMR-5 3/4-inch concrete", Report to the Defense Special Weapons Agency, USAE Waterways Experiment Station, Vicksburg, MS, 1993 (limited distribution).
13. Chen, W.F., and Han, D.J. "Plasticity for structural engineers," Springer – Verlag, New York, 1988
14. Broadhouse, B.J., and Neilson, A.J. "Modeling reinforced concrete structures in DYNA3D," AEEW – M2465, Safety & Engineering Science Division, AEE, Winfrith, October, 1987
15. Algaard, W., Lyle, J., and Izatt, C. "Perforation of composite floors," 5th European LS-DYNA users conference, 25 – 26 May 2005, Birmingham, UK
16. Ottosen N.S. "Failure and elasticity of concrete," RISO – M1801, July, 1975

17. Murray, Y.D., "Users manual for LS-DYNA concrete material model 159," Report No. FHWA-HRT-05-062, Federal Highway Administration, 2007
18. Murray, Y.D., Abu-Odeh, A., and Bligh, R. "Evaluation of concrete material model 159," FHWA-HRT-05-063, June, 2006
19. Rubin, M. "A simple, convenient isotropic failure surface", *ASCE Journal Engineering Mechanics*, vol 117, p 348-369, February, 1991
20. Magallanes, J.M. "Importance of Concrete Material Characterization and Modeling to Predicting the Response of Structures to Shock and Impact Loading," Proceedings of the Tenth International Conference on Structures Under Shock and Impact, Algarve, Portugal, May 13th-15th, 2008
21. Albertsen, N.D. "Influence of compressive strength and wall thickness on behavior of concrete cylindrical hulls under hydrostatic loading", Technical Report, R 790, Naval Civil Engineering Laboratory, Port Hueneme, CA, June 1973
22. Malvar, L.J., and Ross, C.A. "Review of static and dynamic properties of concrete in tension," *ACI Materials Journal*, vol. 95, November-December 1998
23. Comite Euro-International du Beton - Federation Internationale de la Precontrainte, CEB-FIP Model Code 90, Redwood Books, Trowbridge, Wiltshire, Great Britain, 1990 (ISBN 0-7277-1696-4)
24. Clegg, R.A. "Material models for concrete in Hydrocodes - a review of the state-of-the-art", Report R059:01, Century Dynamics Ltd., Dynamics House, West Sussex, England, 3 October 1996
25. Malvar, L.J., Morrill, K.B., and Crawford, J.E. "CTS-1 retrofit designs for reducing the vulnerability of an office building to air blast," Karagozian & Case, TR-98-39.2, Burbank, CA, September, 1998
26. Tsubota, H., Koshika, N., Mizuno, J., Sanai, M., Peterson, B., Saito, H., and Imamura, A. "Scale model tests of multiple barriers against aircraft impact: Part 1. Experimental program and test results," Transactions of the 15th International Conference on Structural Mechanics in Reactor Technology (SMiRT-15), Seoul, Korea, August 15-20, 1999

27.